



ISSN 1335-8871

MEASUREMENT SCIENCE REVIEW

Journal homepage: <https://content.sciendo.com>

## Estimation of Energy Meter Accuracy using Remote Non-invasive Observation

Marius Saunoris<sup>1,2</sup>, Žilvinas Nakutis<sup>1</sup>, Mindaugas Knyva<sup>1</sup>

<sup>1</sup>*Department of Electronics Engineering, Faculty of Electrical and Electronics Engineering, Kaunas University of Technology, Studentu str. 50, LT – 51368, Kaunas, Lithuania, [marius.saunoris@ktu.lt](mailto:marius.saunoris@ktu.lt)*

<sup>2</sup>*Faculty of engineering sciences, Kaunas University of Applied Engineering Sciences, Tvirtovės av. 35, LT – 50155, Kaunas, Lithuania*

**Abstract:** This paper presents an error analysis of the estimation of energy meter correction factor (CF) using a remote non-invasive technique. A method of the CF estimation based on the comparison of synchronously detected power steps in power consumption profiles of meter under test and reference meter is elaborated. The dependence of meter CF estimation uncertainty upon the magnitude of power steps, the number of power steps per observation interval, and the number of meters under test monitored by one reference meter is approximated. The synthesized consumer active power profiles are used to obtain training data points that are fit by these approximating equations.

**Keywords:** Energy meter, accuracy, remote and non-invasive observation.

### 1. INTRODUCTION

Energy meter accuracy is critical seeking to avoid risk cost for both energy consumers and producers [1]. It is typical that metrological precision of meters degrades over time [2]. The in-service conformance assessment of energy meters is regulated by national rules. Metrological verification period (subsequent verification) is country dependent. The cost of verification of all meters is very high and therefore full lot replacement instead of verification is a common practice. Another option is a statistical verification and extension of lot service based on the acceptance rules. In both cases, meters' conformance is not monitored until the expiration of the verification period. Therefore, techniques enabling to monitor the energy meter's accuracy between verifications are in demand [3], [4]. Equipment for in-field verification of energy meters like portable meter testers, portable standards, on-site calibrators, energy meter test sets, etc. are offered by various companies. Disadvantages of in-field verification include the need to visit the customer, transportation of reference equipment, connection to the meter under test and sometimes temporary disconnection of power supply to the customer. On the other hand, the massive roll out of smart meters in distribution grids [5] stimulates research of techniques for the remote metrological maintenance [6]-[12], utilizing communication channels between meters [13]-[17]. In [6], [7], [12], a method based on additional load switching at the meter under inspection is introduced. Another technique described in [8] does not require any additional

load to estimate the calibration status of energy meters using readings of a reference sum meter. However, the method suffers from unreliable error estimates if energy is not consumed at some meters under monitoring in the grid. The further advancement of remote inspection methods based on acquired automatic meter reading data can be seen in [9], [10]. A non-invasive remote monitoring technique introduced in [11] relies on synchronized measurement of power fluctuations due to load switching at the meter under test and sum (reference) meter. In opposite to methods described in [8]-[10], it enables remote inspection of a single meter under test despite the presence of non-technical losses in the grid and accuracy of the rest of meters.

In this paper, we seek to further explore a non-invasive energy meter inspection technique following preliminary findings presented in [11]. The method is adapted to estimate the multiplicative correction factor (CF) of meter under test. The dependence of estimation error of CF on the number of meters under inspection, monitored by a single sum meter, is of interest aiming at reducing the number of necessary sum meters in the segment of distribution grid.

The paper is organized as follows: Section 2 introduces the CF estimation of the energy meter using a non-invasive technique along with two implementation scenarios; Section 3 specifies synthesized power profile data used in modelling. Results of the investigation are presented in Section 4. Finally, the conclusions are presented in Section 5.

## 2. CORRECTION FACTOR ESTIMATION TECHNIQUE

## A. Power steps at reference and meter under monitoring

In the LV AC grid configuration (Fig. 1.), energy meters are connected to the different points of the grid in order to measure the load energy, power consumption, voltage and electrical current. Usually “Total meter” (Fig. 1.) measures the total power of all meters (“Meter n”), which are connected behind it. The typical power profiles acquired by the total meter and another three consumer meters are shown in Fig. 2. The total active power can be expressed as

$$P_T = \sum_{n=1}^{N_m} k_n \cdot P_n, \quad (1)$$

where  $P_T$  is the total active power of all  $n$  consumer loads;  $P_n$  is active power of  $n$ -th consumer load,  $k_n$  is the CF of the  $n$ -th consumer meter,  $N_m$  is the number of consumer meter.

It can be assumed, that the “Total meter” (Fig. 1.) is an accurate (calibrated) energy meter (power meter). However, the accuracy of consumer load connected energy meters is not known. Power steps measured by the “Total meter” and “Meter n” can be exploited for the evaluation of the accuracy of “Meter n”. Certainly, measurements must be performed simultaneously. Two scenarios can be envisaged. The first scenario is based on the utilization of only non-overlapping power steps while the second scenario relies on the application of all power steps (overlapping and non-overlapping).

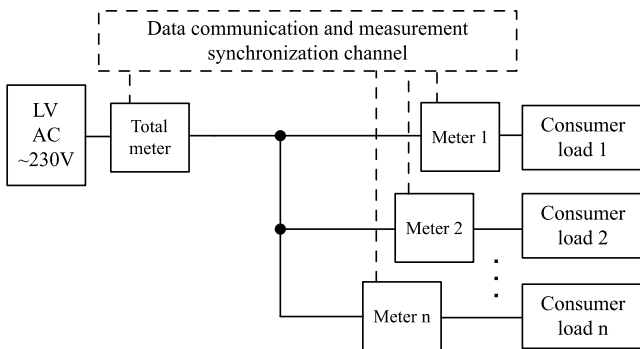


Fig. 1. LV distribution grid and energy meter connections.

The power step can be characterized by its magnitude and time moment of edge occurrence. The threshold for power step magnitude to be used in the CF estimation procedure has to be preset in order to exclude small steps that are buried in noise. To detect a step, the maximal edge duration  $t_e$  of the power step is also set to a chosen value. In this work,  $t_e$  is assumed to be less than five samples when power profile sampling period is 1 second. The minimal speed of the edge rise or fall is set to be not less than 10 W per sampling period. Moreover, the power consumption fluctuations before and after the power step edge are restricted to be less than a threshold level by means of not detecting a power step, which standard deviation of the power fluctuation before and after its edge exceeds by 20 W.

Fig. 2. shows typical power consumption profiles with power steps. These power steps can overlap (1-2 in Fig. 2.) or not overlap (3-8 in Fig. 2.). The overlapping power steps are

such power steps, which appear on two or more consumer loads at the same time moment. In addition, we assume the power steps are overlapping if the following expression holds true:

$$\left( \frac{|\Delta P_T - \Delta P_n|}{\Delta P_T} \right) \cdot 100 \geq 5\%, \quad (2)$$

where  $\Delta P_T$  is the total active power step magnitude measured by the “Total meter”;  $\Delta P_n$  is the active power step magnitude of the particular consumer load.

A comprehensive description of the definition of the power step and of non-overlapping and overlapping power steps can be found in [11].

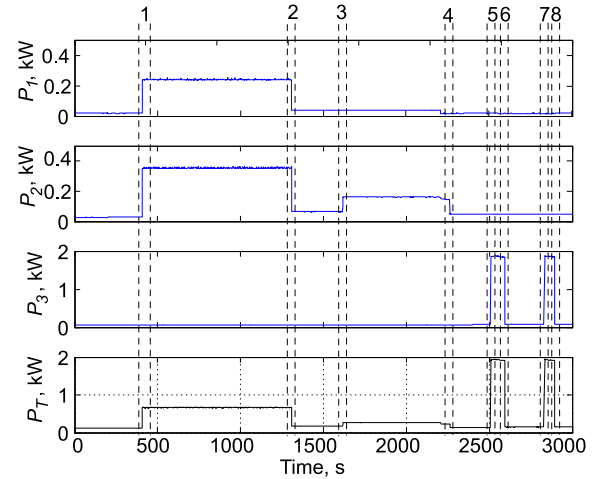


Fig. 2. Typical power profiles of the total meter (lower) and another three consumer meters (upper): 1-2 - overlapping power steps; 3-8 – non-overlapping power steps.

## B. The first implementation scenario

Implementation of the first scenario assumes that only non-overlapping power steps (denote  $N_s^*$ ) are used for the estimation of meter CF. Therefore, CF of the  $n$ -th meter estimated using  $i$ -th power step is defined:

$$k_{ni}^* = \Delta P_{Ti}^* / \Delta P_{ni}^*, \quad (3)$$

where  $\Delta P_{Ti}^*$  is the active power of non-overlapping step measured by the “Total meter”;  $\Delta P_{ni}^*$  is the active power magnitude of the  $i$ -th non-overlapping step measured by the  $n$ -th meter.

Usually, for one consumer load in the given observation interval there is more than one step. Therefore, the averaged CF of the  $n$ -th consumer meter reads:

$$\bar{k}_n^* = \frac{1}{N_s^*} \sum_{i=1}^{N_s^*} k_{ni}^*, \quad (4)$$

where  $N_s^*$  is the number of non-overlapping power steps in the given observation interval;  $\bar{k}_n^*$  is the averaged CF of the  $n$ -th consumer meter.

Averaged CF of all consumer meters that are connected in the particular distribution grid can be defined:

$$\bar{k}^* = \frac{1}{N_m} \sum_{n=1}^{N_m} \bar{k}_n^*. \quad (5)$$

### C. The second implementation scenario

The implementation of the second scenario assumes the utilization of all power steps (denote  $N_s$ ). Some of these power steps are overlapping. Therefore, CF of the n-th meter estimated from the i-th power step is defined:

$$k_{ni} = \Delta P_{Ti} / \Delta P_{ni}, \quad (6)$$

where  $\Delta P_{Ti}$  is the active power of step measured by the ‘‘Total meter’’;  $\Delta P_{ni}$  is the active power magnitude of the i-th step measured by the n-th meter.

In this scenario, the averaged CF of the n-th consumer meter can be defined as

$$\bar{k}_n = \frac{1}{N_s} \sum_{i=1}^{N_s} k_{ni}, \quad (7)$$

where  $N_s$  is the number of all power steps during the period of observation,  $\bar{k}_n$  is the averaged CF of the n-th meter.

In this case, the average CF of all meters can be defined as

$$\bar{k} = \frac{1}{N_m} \sum_{n=1}^{N_m} \bar{k}_n. \quad (8)$$

If all power steps are non-overlapping, the following expression holds true:

$$\bar{k}^* = \bar{k}. \quad (9)$$

### 3. DATA PREPARATION AND MODELING

For the CF error analysis, the synthesized power consumption profile data of individual households generated using the tool LoadProfileGenerator [18], [19] are used. Time resolution (power sampling period) of energy consumption is 1 s. Generated power samples are assigned equal to corresponding meter readings by assuming each meter’s CF is equal to one ( $\bar{k}_{0n}^* = 1$ ;  $\bar{k}_{0n} = 1$ ;  $\bar{k}_0^* = 1$ ;  $\bar{k}_0 = 1$ ; where  $n = 1, 2, 3, \dots$ ). The total load profile is obtained by summing up load profiles of all synthesized household consumptions. In this preliminary analysis, distribution line losses are neglected.

The corresponding relative errors of the evaluation of the CF can be expressed as

$$\delta \bar{k}_n^* = \frac{\bar{k}_n^* - \bar{k}_{0n}^*}{\bar{k}_{0n}^*} \cdot 100 \text{ [%]}, \quad (10)$$

$$\delta \bar{k}_n = \frac{\bar{k}_n - \bar{k}_{0n}}{\bar{k}_{0n}} \cdot 100 \text{ [%]}, \quad (11)$$

$$\delta \bar{k}^* = \frac{\bar{k}^* - \bar{k}_0^*}{\bar{k}_0^*} \cdot 100 \text{ [%]}, \quad (12)$$

$$\delta \bar{k} = \frac{\bar{k} - \bar{k}_0}{\bar{k}_0} \cdot 100 \text{ [%]}, \quad (13)$$

where  $\delta \bar{k}_n^*$  is the relative error of the CF estimation of each consumer load meter (non-overlapping power steps are used in CF estimation);  $\delta \bar{k}_n$  is the relative error of the CF estimation of each consumer load meter (all power steps are used in CF estimation);  $\delta \bar{k}^*$  is the relative error of the

averaged CF estimation of all consumer meters (non-overlapping power steps are used for the calculations);  $\delta \bar{k}$  is the relative error of the estimation of averaged CF of all consumer meters (all power steps are used for the calculations).

### 4. RESULTS

As it can be seen from Fig.3., the non-overlapping power steps (denoted by  $N_s^*$ ) comprise only a small fraction of all power steps. It is obvious that the number of power steps is linearly proportional to the observation period in the synthesized power profiles that were used in the following analysis.

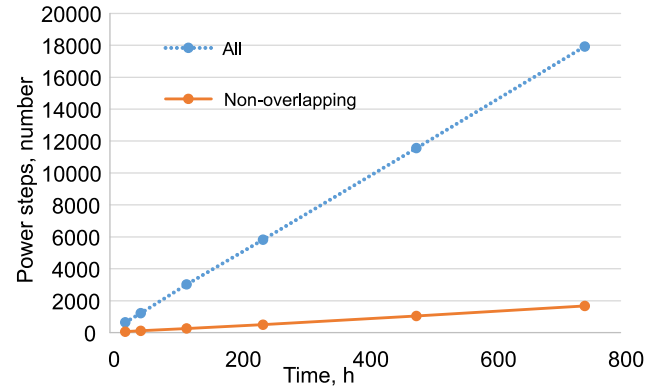


Fig.3. Relationship between time interval of power profile and sum of power steps ( $\Delta P_n \geq 100$  W, the number of grid meters is 30).

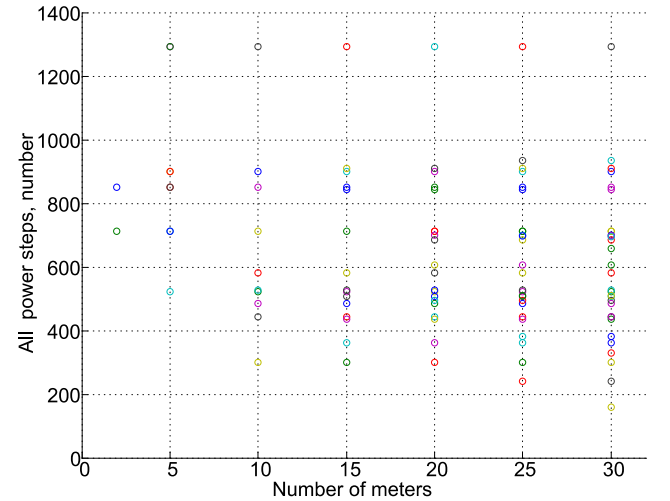


Fig.4. The scatter diagram of the number of power steps at each meter (different dot color denotes different meter). The time interval of power profile is 744 hours = 31 days = 1 month, only power steps with the magnitude not less than 100 W are detected.

The distribution of all power steps  $N_s$  among every meter is presented in Fig.4. Each point in Fig.4. shows how many steps were detected at the n-th meter in the grid. It can be seen that the number of steps detected by each meter is strongly scattered. Fig.5. shows a distribution of non-overlapping power steps at every meter. If the number of meters in the grid increases, the number of non-overlapping power steps considerably decreases.

From the results presented in Table 1. it is evident that smaller power loads switching dominates in the power consumption profile. Analysis of power steps (Table 1.) shows that a large part of the small magnitude power steps is overlapping. Therefore, in order to detect non-overlapping power steps, it is advisable to employ the range of higher magnitude power steps.

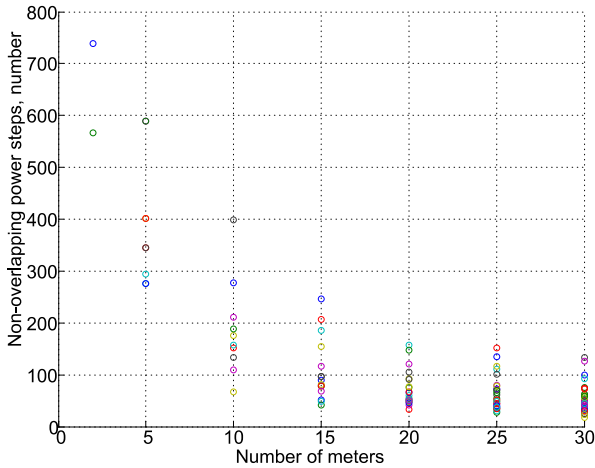


Fig.5. The scatter diagram of non-overlapping power steps at each meter. The time interval of power profile is 744 hours, only power steps with the magnitude not less than 100 W are detected.

The estimation error of the CF of each consumer meter depends on the number of grid meters, on the number of power steps, and on the magnitude of power steps. The statistical analysis reveals that using only non-overlapping power steps yields lower errors. Fig.6. shows the distribution of the estimation error of the CF per meter.

The statistical analysis also reveals that using all power steps instead of only non-overlapping steps, yields higher estimation error of the CF per meter. The increasing number of grid meters causes the higher level of overlapping. The distribution of the estimation error of the CF of each meter when all power steps are used for the evaluation is presented in Fig.7.

The averaged parameters  $\delta\bar{k}^*$ ,  $\delta\bar{k}$  and their standard errors  $SE_{\delta\bar{k}^*}$ ,  $SE_{\delta\bar{k}}$  of grid meters are used for the comparison. Table 2. shows that using only non-overlapping power steps the obtained estimation error of the averaged CF of all meters almost does not depend upon the number of meters (or consumer loads) in the grid. However, utilizing all power

steps results in the obvious relationship between the number of meters in the grid and estimation error of the meter's CF. Standard errors are significant for the estimation error of the averaged CF when using all power steps.

The number of detected power steps also influences the estimation error of the averaged CF (see Table 3.). The strong influence can be observed if all power steps are used. Note that the variation of the values of standard error of the estimation error of the averaged CF ( $SE_{\delta\bar{k}^*}$ ) is much less when non-overlapping power steps are used.

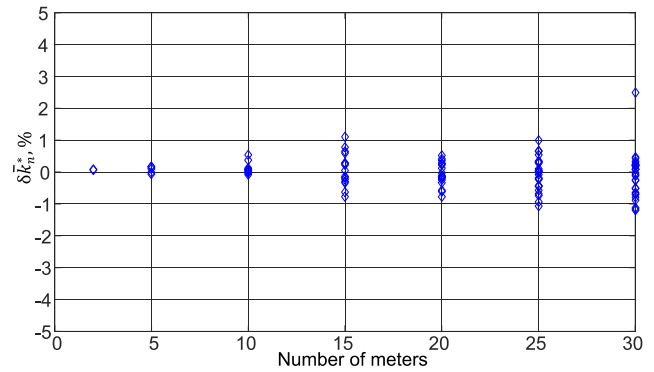


Fig.6. The distribution of the estimation error of the CF of each (n) meter (only non-overlapping power steps are used, the time interval of power profile is 744 hours,  $\Delta P_n \geq 300$  W).

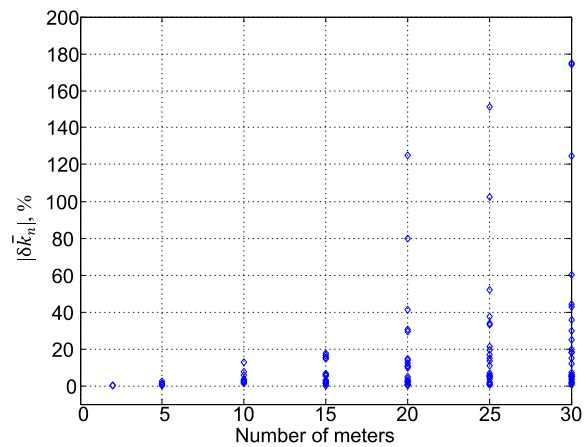


Fig.7. The distribution of the estimation error of the CF of each (n) meter (all power steps are used, the time interval of power profile is 744 hours,  $\Delta P_n \geq 300$  W).

Table 1. The relationship between number of power steps and the magnitude of power steps (the observation interval is 240 hours (10 days)).

Number of meters	$\Delta P_n=(100\div 300)$ [W]		$\Delta P_n=(300\div 500)$ [W]		$\Delta P_n=(500\div 1000)$ [W]		$\Delta P_n\geq 1000$ [W]	
	$N_s$	$N_s^*$	$N_s$	$N_s^*$	$N_s$	$N_s^*$	$N_s$	$N_s^*$
2	208	145	54	48	168	148	74	71
5	618	159	132	47	427	223	178	133
10	1088	167	186	57	602	201	255	135
15	1669	162	321	72	759	139	387	128
20	2441	166	409	48	836	116	478	119
25	3047	208	478	47	964	121	610	152
30	3418	185	537	44	1184	122	684	143

Table 2. The relationship between the estimation error of the averaged CF of all meters and the number of meters ( $\Delta P_n \geq 300W$ , the observation interval is 240 hours).

$N_m$	$ \delta\bar{k}^* , [\%]$	$SE_{\delta\bar{k}^*}, [\%]$	$ \delta\bar{k} , [\%]$	$SE_{\delta\bar{k}}, [\%]$
2	0.059	0.805	0.043	0.309
5	0.104	1.039	1.246	0.897
10	0.434	0.801	5.792	3.300
15	0.002	0.690	5.744	2.829
20	0.255	0.613	19.801	7.685
25	0.020	0.569	20.862	7.633
30	0.073	0.516	30.807	9.553

When solving a problem of selection of number of meters and a number of steps to acquire in order to achieve the best accuracy of the CF estimate, the uncertainty should be considered the target. The uncertainty of the CF estimate includes both averaged error (absolute shift) and its standard error:

$$u(\delta\bar{k}) = \sqrt{(\delta\bar{k})^2 + (SE_{\delta\bar{k}})^2}. \quad (14)$$

To derive mathematical approximation of the uncertainty relationship to the number of power steps  $N_s$  and different number of meters  $N_m$ , the following steps are completed:

1. Synthesizing of power consumption profiles of different consumers are performed using the open source tool LoadProfileGenerator [18]. These profiles are accepted as readings of a corresponding customer load meter by setting the CF equal to 1.0.

2. Estimations of the CF of each meter according to (10) or (11) are made using the proposed detection of power steps in power consumption profiles.
3. The averaging of CFs ((12), (13)) and the calculations of the uncertainties of the estimations of CF of each meter is conducted according to (14).
4. Data points consisting of three coordinates (uncertainty, number of meters, and number of steps) are approximated in order to model the function (see Table 4.)

$$u(\delta\bar{k}) = \hat{u} = F(N_m, N_s) \quad (15)$$

by applying Matlab function of Curve Fitting Tool.

It is found that linear approximation fits the obtained data representing samples of (15) well, according to the R-square (the coefficient of multiple determination) shown in Fig.8.-Fig.10.

Analytical relationships (Table 4., Fig.8.-Fig.10.) may be used to choose the combination of uncertainty, number of grid meters and number of power steps required to complete the CF estimation procedure. A good fit to linear approximation of the function (15) indicates that in the range of explored  $N_m$  and  $N_s$  their optimal values do not exist. Indeed, the larger is the number of power steps  $N_s$ , the less is uncertainty due to more averaged items. Also, the larger is the number of meters  $N_m$  in the grid, the uncertainty tends to increase because of negative influence of larger number of overlapping power steps.

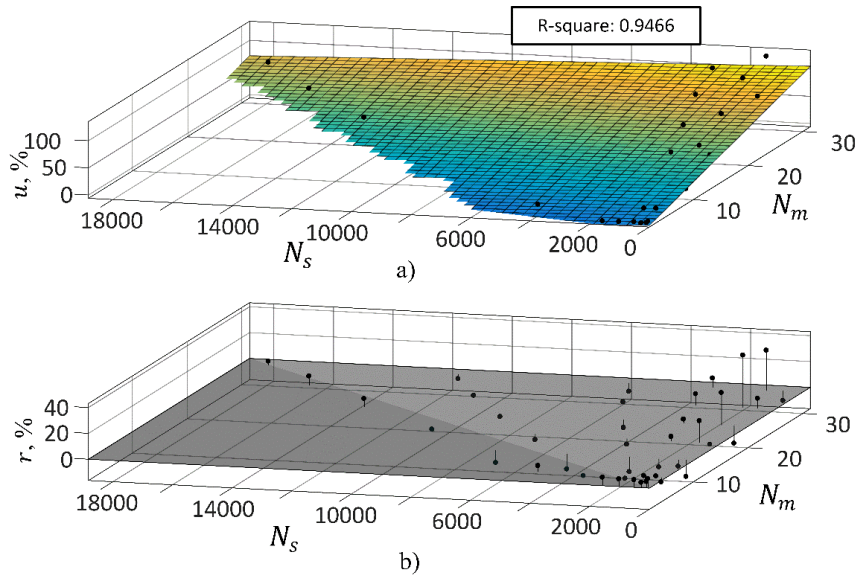


Fig.8. a) Approximation of the relationship  $\hat{u} = F(N_m, N_s)$  ( $\Delta P_n \geq 100 W$ ); b) Residuals plot, where  $r = u - \hat{u}$ ,  $\hat{u}$  – predicted value of  $u$ .

Table 3. The relationship between the estimation error of the averaged CF of 10 meters and the number of power steps ( $\Delta P_n \geq 500 W$ ).

Observation interval, h	$ \delta\bar{k}^* , [\%]$	$SE_{\delta\bar{k}^*}, [\%]$	$ \delta\bar{k} , [\%]$	$SE_{\delta\bar{k}}, [\%]$	$N_s^*$	$N_s$
24	0.53	0.81	6.83	1.70	40	95
48	0.37	0.85	2.30	1.89	73	183
120	0.29	0.83	1.88	1.38	171	456
480	0.11	0.80	1.38	0.63	691	1698
744	0.16	0.79	1.30	0.56	1148	2708

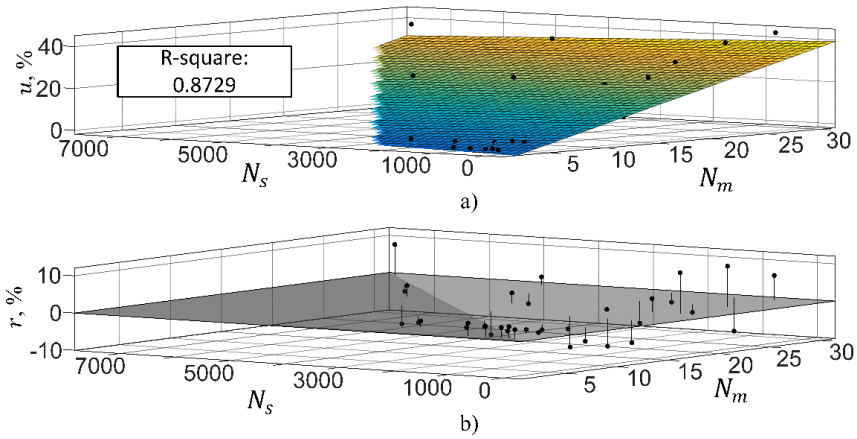


Fig.9. a) Approximation of the relationship  $\hat{u} = F(N_m, N_s)(\Delta P_n \geq 300 \text{ W})$ ; b) Residuals plot, where  $r = u - \hat{u}$ ,  $\hat{u}$  – predicted value of  $u$ .

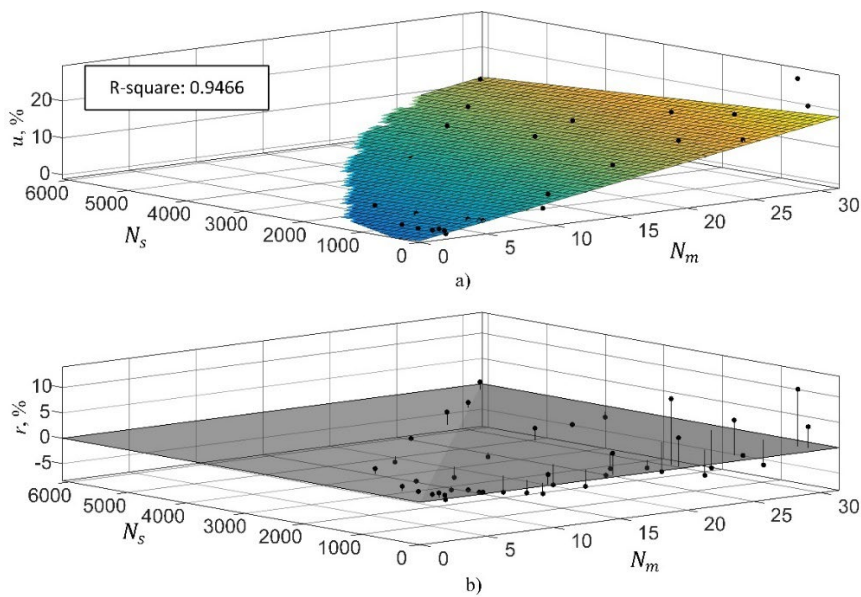


Fig.10. a) Approximation of the relationship  $\hat{u} = F(N_m, N_s)(\Delta P_n \geq 500 \text{ W})$ ; b) Residuals plot, where  $r = u - \hat{u}$ ,  $\hat{u}$  – predicted value of  $u$ .

Table 4. Approximations of the uncertainty of averaged CF estimation (the observation interval is 744 hours).

$\Delta P_n$ threshold	$\hat{u}=F(N_m, N_s)$	Fig.
$\geq 100\text{W}$	$\hat{u}=-10.43+3.688 \cdot N_m-0.001793 \cdot N_s$ [%]	8
$\geq 300\text{W}$	$\hat{u}=14.61+13.61 \cdot N_m-1.876 \cdot N_s$ [%]	9
$\geq 500\text{W}$	$\hat{u}=7.209+5.826 \cdot N_m-1.512 \cdot N_s$ [%]	10

5. CONCLUSIONS

Uncertainty analysis of energy meter correction factor estimation using the introduced remote non-invasive technique is performed utilizing synthesized power consumption profiles.

It is found that the uncertainty can be reduced by acquiring more power samples (negative linear coefficient in the approximating equation) and by attributing a sum meter to monitor less meters under inspection (positive linear coefficient in the approximating equation). In opposite to the initial expectations, any optimal number of meters minimizing the correction factor uncertainty was not identified. When the number of meters inspected using a single sum reference meter increases, the larger percentage of occurrence moments of all power steps taking place in the

grid due to customer loads switching tends to overlap. More overlapping power steps seem to cause the growth of uncertainty despite the expectation that different overlapping directions (up and down steps) will suppress each other's influence in the averaging process. Considering up to 30 meters grouped with a sum meter, the obtained results did not reveal anything but linear growth of the uncertainty in response to the increase of number of meters. Nevertheless, the approximated empirical relationship between the correction factor uncertainty and both numbers of detected steps and meters monitored by a sum meter, provides means to select combinations of the number of steps to acquire and the number of meters seeking to meet requirements for the estimation uncertainty.

## REFERENCES

- [1] Li, N., Yang, J., Sun, Y., Wang, G., Zhang, J., Liu, C. (2018). Failure modes and effects analysis for domestic electric energy meter using in-service data. *IOP Conference Series: Earth and Environmental Science (EES)*, 108 (5), 052036. <https://doi.org/10.1088/1755-1315/108/5/052036>
- [2] Yang, Z., Chen, Y.X., Li, Y.F., Zio, E., Kang, R. (2014). Smart electricity meter reliability prediction based on accelerated degradation testing and modeling. *International Journal of Electrical Power & Energy Systems*, 56, 209-219. <https://doi.org/10.1016/j.ijepes.2013.11.023>
- [3] Nakutis, Ž., Kaškonas, P., Saunoris, M., Daunoras, V., Jurčević, M. (2021). A framework for remote in-service metrological surveillance of energy meters. *Measurement*, 168, 108438. <https://doi.org/10.1016/j.measurement.2020.108438>
- [4] Nakutis, Ž., Kaškonas, P. (2020). A contemplation on electricity meters in-service surveillance assisted by remote error monitoring. *Energies*, 13 (20), 5245. <https://doi.org/10.3390/en13205245>
- [5] European Commission. (2018). *Smart grids and meters*. [https://ec.europa.eu/energy/topics/markets-and-consumers/smart-grids-and-meters/overview\\_en?redir=1](https://ec.europa.eu/energy/topics/markets-and-consumers/smart-grids-and-meters/overview_en?redir=1)
- [6] Nakutis, Ž., Saunoris, M., Ramanauskas, R., Daunoras, V., Lukočius, R., Marčiulionis, P. (2019). A method for remote estimation of wattmeter's adjustment gain. *IEEE Transactions on Instrumentation and Measurement*, 68 (3), 713-721. <https://doi.org/10.1109/TIM.2018.2857118>
- [7] Lukočius, R., Nakutis, Ž., Daunoras, V., Deltuva, R., Kuzas, P., Račkienė, R. (2019). An analysis of the systematic error of a remote method for a wattmeter adjustment gain estimation in smart grids. *Energies*, 12 (1), 37. <https://doi.org/10.3390/en12010037>
- [8] Seppa, H. (2007). *Method and system for the calibration of meters*. WO 2007/063180 A1, Patent Cooperation Treaty (PCT). <http://www.freepatentsonline.com/WO2007063180.html>
- [9] Kong, X., Ma, Y., Zhao, X., Li, Y., Teng, Y. (2019). A recursive least squares method with double-parameter for online estimation of electric meter errors. *Energies*, 12 (5), 805. <https://doi.org/10.3390/en12050805>
- [10] Liu, F., Liang, C., He, Q. (2020). Remote malfunctioned smart meter detection in edge computing environment. *IEEE Access*, 8, 67436-67443. <https://doi.org/10.1109/ACCESS.2020.2985725>
- [11] Nakutis, Ž., Rinaldi, S., Kuzas, P., Lukočius, R. (2020). A method for noninvasive remote monitoring of energy meter error using power consumption profile. *IEEE Transactions on Instrumentation and Measurement*, 69 (9), 6677-6685. <https://doi.org/10.1109/TIM.2020.3002402>
- [12] Daunoras, V. (2021). *A method for remote monitoring of electrical energy meter errors*. Thesis, Kaunas University of technology, Kaunas, Lithuania. <https://en.ktu.edu/events/v-daunoras-a-method-for-remote-monitoring-of-electrical-energy-meter-errors-doctoral-dissertation-defence/>
- [13] Abate, F., Carratu, M., Liguori, C., Paciello, V. (2019). A low cost smart power meter for IoT. *Measurement*, 136, 59-66. <https://doi.org/10.1016/j.measurement.2018.12.069>
- [14] Artale, G., Cataliotti, A., Cosentino, V., Di Cara, D., Fiorelli, R., Guaiana, S., Panzavecchia, N., Tine, G. (2018). A new PLC-based smart metering architecture for medium/low voltage grids: Feasibility and experimental characterization. *Measurement*, 129, 479-488. <https://doi.org/10.1016/j.measurement.2018.07.070>
- [15] Avancini, D.B., Rodrigues, J.J.P.C., Martins, S.G.B., Rabelo, R.A.L., Al-Muhtadi, J., Solic, P. (2019). Energy meters evolution in smart grids: A review. *Journal of Cleaner Production*, 217, 702-715. <https://doi.org/10.1016/j.jclepro.2019.01.229>
- [16] Matanza, J., Alexandres S., Rodríguez-Morcillo, C. (2014). Advanced metering infrastructure performance using European low-voltage power line communication networks. *IET Communications*, 8 (7), 1041-1047. <https://doi.org/10.1049/iet-com.2013.0793>
- [17] Bat-Erdene, B., Lee, B., Kim, M.-Y., Ahn, T.H., Kim, D. (2013). Extended smart meters-based remote detection method for illegal electricity usage. *IET Generation, Transmission & Distribution*, 7 (11), 1332-1343. <https://doi.org/10.1049/iet-gtd.2012.0287>
- [18] Pflugradt, N. (2021). *Load profile generator*. <https://www.loadprofilegenerator.de>
- [19] Pflugradt, N., Teuscher, J., Platzer, B., Schufft, W. (2013). Analysing low-voltage grids using a behaviour based load profile generator. In *Renewable Energy & Power Quality Journal*, 1 (11), 361-365. <https://doi.org/10.24084/repqj11.308>

Received September 27, 2021

Accepted March 28, 2022